Blackwell Publishing

TRPM and TRPV in rat prostate
DOI: 10.1111/j.1745-7262.2007.00291.x

AJA
www.asiaandro.com

·*Original Article*·

Distribution profiles of transient receptor potential melastatin-related and vanilloid-related channels in prostatic tissue in rat

Huai-Peng Wang*, Xiao-Yong Pu*, Xing-Huan Wang

Department of Urology, Guangdong Provnicial People's Hospital, Guangzhou 510080, China

Abstract

Aim: To investigate the expression and distribution of the members of the transient receptor potential (TRP) channel members of TRP melastatin (TRPM) and TRP vanilloid (TRPV) subfamilies in rat prostatic tissue. **Methods:** Prostate tissue was obtained from male Sprague-Dawley rats. Reverse transcription polymerase chain reaction (RT-PCR) and quantitative real-time polymerase chain reaction (PCR) were used to check the expression of all TRPM and TRPV channel members with specific primers. Immunohistochemistry staining for TRPM8 and TRPV1 were also performed in rat tissues. **Results:** TRPM2, TRPM3, TRPM4, TRPM6, TRPM7, TRPM8, TRPV2 and TRPV4 mRNA were detected in all rat prostatic tissues. Very weak signals for TRPM1, TRPV1 and TRPV3 were also detected. The mRNA of TRPM5, TRPV5 and TRPV6 were not detected in all RT-PCR experiments. Quantitative real-time RT-PCR showed that TRPM2, TRPM3, TRPM4, TRPM8, TRPV2 and TRPV4 were the most abundantly expressed TRPM and TRPV subtypes, respectively. Fluorescence immunohistochemistry indicated that TRPM8 and TRPV1 are highly expressed in both epithelial and smooth muscle cells. **Conclusion:** Our results demonstrate that mRNA or protein for TRPM1, TRPM2, TRPM3, TRPM4, TRPM6, TRPM7, TRPM8, TRPV1, TRPV2, TRPV3 and TRPV4 exist in rat prostatic tissue. The data presented here assists in elucidating the physiological function of TRPM and TRPV channels. *(Asian J Androl 2007 Sep; 9: 634–640)*

Keywords: transient receptor potential channels; prostate; cation channels

1 Introduction

Prostate cancer is the most commonly diagnosed cancer in US men and its incidence rate is steadily rising in China [1]. It is possible to effectively treat organ-confined prostate cancer by radical prostatectomy and radiation therapy [2]. Targeted-cryosurgical ablation of the prostate with androgen deprivation therapy improves the quality of life for high-risk prostate cancer patients.

Correspondence to: Dr Xing-Huan Wang, Department of Urology, Guangdong Provincial People's Hospital, Guangzhou 510080, China.
Tel: +86-20-8382-7812 Fax: +86-20-8382-7712
E-mail: urologist@126.com
*The authors equally contribute to the study and preparation of the manuscript.
Received 2006-11-19 Accepted 2007-04-04

However, there are very limited treatment options for metastatic prostate cancer. Therefore, it is of great importance to find novel markers for diagnosing early stages of the disease and to closely monitor both progression and treatment of the disease, as well as to develop new therapeutic approaches. To achieve this, we need to screen candidate molecules for biomarkers and compare their expression in normal prostatic tissue and neoplastic tissue. To date, there are very few prostate-specific markers available. The best-known and most well-characterized markers for prostate cancer are prostate specific antigen (PSA) [3] and prostate-specific membrane antigen (PSMA) [4]. Each of these proteins has also become the target for novel immunotherapy approaches to the treatment of the disease [5, 6].

The transient receptor potential (TRP) channels, have not yet been systematically studied in prostate even though some subfamilies have been explored. The TRP protein superfamily consists of a diverse group of cation channels that bear structural similarities to *Drosophila* TRP. Based on sequence homology, the TRP superfamily can be divided into three major subfamilies of canonical (TRPC), melastatin-related (TRPM) and vanilloid-related (TRPV) channels and into four more distant subfamilies of polycystin (TRPP), mucolipin (TRPML), ankyrin (TRPA), and no mechanoreceptor potential C or NOMPC (TRPN)-related channels/proteins. Of all the TRP superfamily, only the TRPC subfamily is a store-operated channel, whereas others appear to be activated by production of diacylglycerol or regulated through an exocytotic mechanism. Many members of TRPV function in sensory physiology and respond to heat, changes in osmolarity, odorants and mechanical stimuli. Two members of the TRPM family function in sensory perception and three TRPM proteins are chanzymes, which contain C-terminal enzyme domains. As for TRPN and TRPA, the proteins are characterized by many ankyrin repeats. TRPN proteins function in mechanotransduction, whereas TRPA1 is activated by noxious cold and is also required for auditory response. In addition to these five closely related TRP subfamilies, which comprise the Group 1 TRP, members of the two Group 2 TRP subfamilies, TRPP and TRPML, are distantly related to the Group 1 TRP. Mutations in the found members of these latter subfamilies are responsible for human diseases [7].

In the present study, we systematically analyzed the expression of TRPM and TRPV channels, two important subfamilies of the TRP superfamily, in rat prostate. Perhaps of the greatest interest is the observation that some TRP channels appear to be expressed in a large spectrum of normal prostate tissue. Some might potentially be used as markers in prostate cancer diagnosis and for monitoring disease progression during treatment.

2 Materials and methods

2.1 Rat tissue

Care of animals conformed to standards established by the National Institute of Health of China. The Guangdong Provincial People's Hospital Animal Care and Use Committee approved all animal protocols. Three-month-old Sprague-Dawley rats were killed with pentobarbital sodium (130 mg/kg i.p.). They were exsanguinated, and the prostate were isolated and removed quickly. The prostate was cleaned free of connective tissue.

2.2 Reverse transcription reaction (PCR)

The prostate tissue was obtained and maintained at –80ºC until processing for mRNA expression analysis. Total RNA was extracted using TRIzol reagent (Invitrogen, Carlsbad, CA, USA) from the prostate tissue using the standard procedures. In a 20-μL reaction 1 μg of total RNA was resuspended in dihexadecylphosphatidylcholine (DEPC)-treated water. The reverse transcription (RT) reaction was performed using an RT system procedure (Promega, Madison, USA). Briefly, 5 mmol/L $MgCl_2$, 1 × RT buffer (10 mmol/L tris-HCl, 50 mmol/L KCl and 0.1% Triton X-100), 1 mmol/L deoxynucleoside triphosphate (dNTP) mixture (equal amounts of deoxyadenosine triphosphate [dATP], deoxycytidine triphosphate [dCTP], deoxyguanosine triphosphate [dGTP] and deoxythymidine triphosphate [dTTP]) (Sigma-Aldrich), 1 μg/μL recombinant RNase (Jingmei Biotech, Shenzhen, China) ribonuclease inhibitor, 15 U avian myeloblastosis virus (dAMV) RT (high concentration) and 0.5 μg oligodeoxythymidine (oligo DT) 15 primers were added to the RNA mixture. The reaction was done at 37ºC for 5 min and 42ºC for 1 h, followed by 10 min of heating at 95ºC to destroy the enzyme and RNA.

2.3 Conventional PCR amplification

Sense and anti-sense PCR primers specific to the TRPM and TRPV channels were designed as Yang *et al.* [8]. RT reaction (1 μL) was amplified in a 20-μL reaction containing 1 × PCR buffer, 0.5 unit Taq (Promega,

Madision, NJ, USA) DNA polymerase, 0.25 mmol/L dNTP mixture (equal amounts of dATP, dCTP, dGTP and dTTP), 0.2 mmol/L sense and antisense primers, and 0.25 μL dimethyl sulfoxide (DMSO). Cycle parameters consisted of a 30-s denaturing step at 94ºC, 45-s annealing step at 56ºC and 90-s extension step at 72ºC with 35 cycles per amplification. This was followed by a final extension at 72ºC for 10 min and the products were then stored at 4ºC. PCR products were electrophoresed on 1.8% agarose gel (Jingmei Biotech, Shenzhen, China), stained with 0.5 μg/mL ethidium, and visualized and photographed on an ultraviolet transilluminator bromide (SIM International, Los Angeles, CA, USA). Parallel reactions were run for each RNA sample in the absence of Superscript III to ascertain that there was no genomic DNA contamination.

2.4 Quantitative real-time PCR

Gene-specific real-time PCR primers were designed based upon the published TRPM or TRPV sequences in Genbank to obtain predicted PCR products of 100–150 bases. At least one primer of each set was designed to span exon-exon junctions in order to minimize the possibility of amplifying the genomic DNA. PCR reactions were performed with QuantiTect SYBR Green PCR Master Mix (Qiagen, Valencia, CA, USA), using 2 μL of cDNA as the template in each 25 μL reaction mixture. PCR assays were performed with an MJ Research Chrom4 Thermal Cycler System (MJ Research, Waltham, MA, USA). The PCR protocol consisted of initial enzyme activation at 95ºC for 15 min, followed by 40 cycles at 95ºC for 15 s and 60ºC for 1 min. Using the same protocol, standard curves were generated from serial dilutions of purified PCR products with known copy numbers measured by absorbance at 260 nm. The absolute copy number of mRNA of interest was determined by interpolation of the standard curve with the threshold cycle value of each sample. To confirm the specificity of PCR products, a melting curve was obtained at the end of each run by slow heating with 0.1ºC/s increments from 65ºC to 95ºC, with fluorescence detected at 0.1ºC intervals. Standard gel electrophoresis was also performed to ensure that the end product generated a single band with the predicted size (100–150 bases). Data were also normalized with the quantity of 18S rRNA in individual samples to correct for sample variability.

2.5 Immunohistochemistry staining

Indirect immunohistochemistry staining was performed using the conventional procedure. The primary antibodies were the same as those used for the Western blot. Briefly, paraffin section slides were de-paraffinated with 100% xylenes for three times, each time for 5 min, then the sections were rehydrated with 100%, 85% and 70% alcohol. Slides were placed in PBS for 5 min, and antigen retrieval was done by covering the sections with 0.02 mol/L citrate buffer, pH 6.0, and heating them in a microwave oven for 3 min. After cooling for 3 min, additional buffer was added and slides were reheated. This process was repeated until four cycles of heating and cooling had been performed. Slides were cooled down to room temperature for 20 min, rinsed with PBS and blocked with 8% normal goat serum in PBS for 45 min. The sections were incubated overnight at 4ºC with primary antibody containing 3% serum. After washing three times with PBS/0.05% Tween-20 (PBST), sections were incubated for 1 h at room temperature with Cy3-conjugated goat anti-rabbit antibody (1:800, Jackson Immunolab, West Grove, USA). Sections were thoroughly washed with PBST, and then counterstained with the nuclear dye Hoechest 32258 (1:1 200, Sigma; St. Louis, MO, USA). Slides were mounted with Aquamount solution and viewed with a Nikon Fluorescence Microscope (Nikon Instruments, NY, USA). Images were captured using a Nikon digital camera and SOP RT 3.4 software (Nikon, Tokyo, Japan). Pictures were obtained by merging the image of a Hoechst-stained slide and the fluorescence image from the same field.

3 Results

3.1 Expression of TRPM/TRPV channels mRNA

Figures 1 and 2 shows amplified products using conventional RT-PCR from prostate tissue of rats. PCR products of TRPM2, TRPM3, TRPM4, TRPM6, TRPM7, TRPM8, TRPV1, TRPV2, and TRPV4 were obtained consistently in four separate experiments. Much weaker bands for TRPM1 and TRPV3 were also determined. All these RT-PCR amplified products had sizes corresponding to the predicted values. The bands of TRPM5, TRPV5 and TRPV6 were not detected completely in all experiments.

3.2 Quantification of TRPM and TRPV mRNA

The relative expression of TRPM and TRPV mRNA was determined by quantitative real-time RT-PCR.

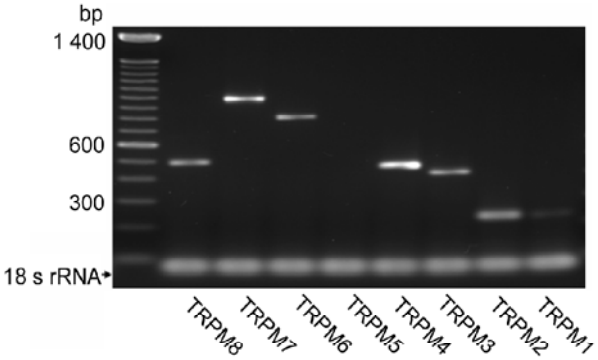

Figure 1. Conventional reverse transcriptase polymerase chain reaction (RT-PCR) analysis of transient receptor potential melastatin (TRPM) subtypes in rat prostatic tissue. Predicted lengths of PCR products are 228, 232, 425, 443, 790, 978 and 489 bp for TRPM1, TRPM2, TRPM3, TRPM4, TRPM6, TRPM7 and TRPM8, respectively. All the objective bands were detected, except the 267 bp band associated with TRPM5.

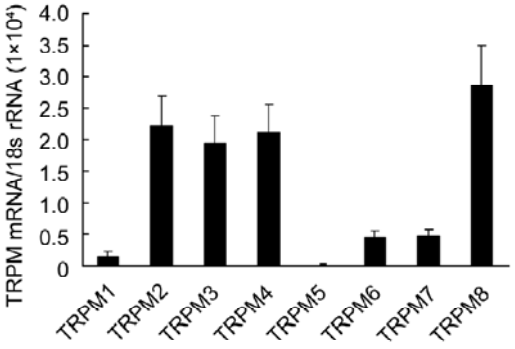

Figure 3. Real-time reverse transcriptase polymerase chain reaction (RT-PCR) analysis of the relative expression of transient receptor potential melastatin (TRPM) mRNA in rat prostatic tissue. Data are expressed as a percentage normalized to 18S rRNA to correct for RNA quantity and integrity. TRPM8 is the most abundant TRPM subtype, and TRPM2, TRPM3 and TRPM4 are also highly expressed. Five animals were used for each channel subtype.

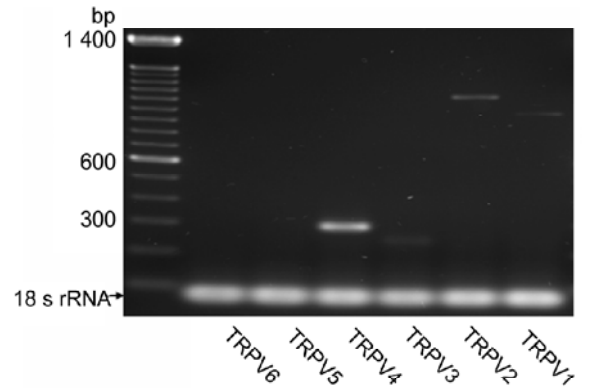

Figure 2. Reverse transcriptase polymerase chain reaction (RT-PCR) analysis of transient receptor potential vanilloid (TRPV) subtypes in rat prostatic tissues. Predicted lengths of PCR products are 964, 1131, 233, and 287 bp for TRPV1, TRPV2, TRPV3 and TRPV4, respectively.

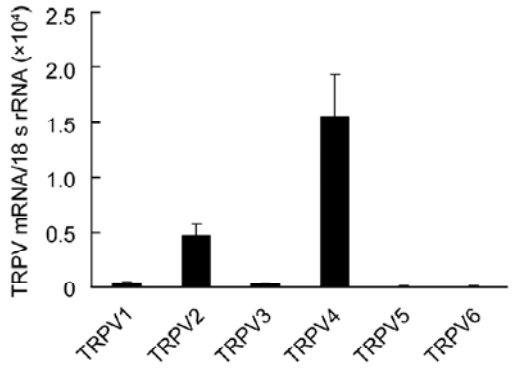

Figure 4. Real-time reverse transcriptase polymerase chain reaction (RT-PCR) analysis of the relative expression of transient receptor potential melastatin (TRPM) mRNA in rat prostatic tissue. Data are expressed as percentage normalized to 18S rRNA to correct for RNA quantity and integrity. TRPV4 is the most abundant TRPV subtype. Five animals were used for each preparation.

TRPM8 expression was the highest among all TRPM subtypes in rat prostatic tissue, with levels equivalent to 0.0284 ± 0.0064% of 18S rRNA (Figure 3). TRPM2, TRPM3 and TRPM4 were also highly expressed but less than TRPM8, approximately equal to 71%, 69% and 68% of TRPM8, respectively. In contrast, TRPM1, TRPM6 and TRPM7 transcripts were expressed at less than 2.5%, 14.0% and 16.5% of TRPM8, whereas the expression of TRPM5 mRNA were exceedingly low even though their products were detectable. Overall, the expression of TRPM channels are in the order of:

TRPM8 > TRPM2 > TRPM4 > TRPM3 > TRPM7 > TRPM6 > TRPM1 > TRPM5.

For the TRPV subfamily, TRPV4 mRNA was most abundantly expressed, being equivalent to 0.0155 ± 0.0038% of 18S rRNA (Figure 4). It was followed by TRPV2, which was only approximately 3% TRPV4. The TRPV1 and TRPV3 were expressed by even less, at 0.3% and 0.2% of TRPV4. The TRPV5 and TRPV6 were the least expressed among the detected TRPV channels and were

almost undetectable. The expression of TRPV transcripts are in the order of:

TRPV4 > TRPV2 > TRPV1 > TRPV3 > TRPV5 > TRPV6.

Experiments with samples from five different animals were performed for the quantification of each channel subtype.

3.3 Expression and localization of TRPM and TRPV proteins

Figure 5 shows the expression and localization of TRPM8 and TRPV1 in rat prostate tissues by fluorescence immunohistochemistry. Clearly, positive staining was noted in both epithelial and smooth muscle cells. The highest TRPM8 and TRPV1 protein expressions were localized in cytoplasm and cell membranes (Figures 5A and 5C).

4 Discussion

The expression and function of some members of the TRPM and TRPV subfamilies are poorly understood and still mysterious in prostatic tissue. For the first time, we systematically studied the expression of TRPM and TRPV channels in rat prostatic tissue. The study showed that: (i) multiple TRPM and TRPV channel subtypes are co-expressed in rat prostatic tissue; (ii) TRPM8, TRPM2, TRPM4 and TRPM3 mRNA are most abundantly expressed among the TRPM members, whereas TRPV2 and TRPV4 mRNA are the predominant TRPV transcripts.

The systematic analysis of TRPM and TRPV expression clearly demonstrates at mRNA levels that multiple TRPM and TRPV channels are co-expressed in prostatic tissue of rat. TRPM8 was abundant expression in the normal prostatic tissue in the present and in other studies [9]. It is demonstrated that the TRPM8 channel is expressed in both epithelial and smooth muscle cells in rat prostatic tissues, which is in accordance with the

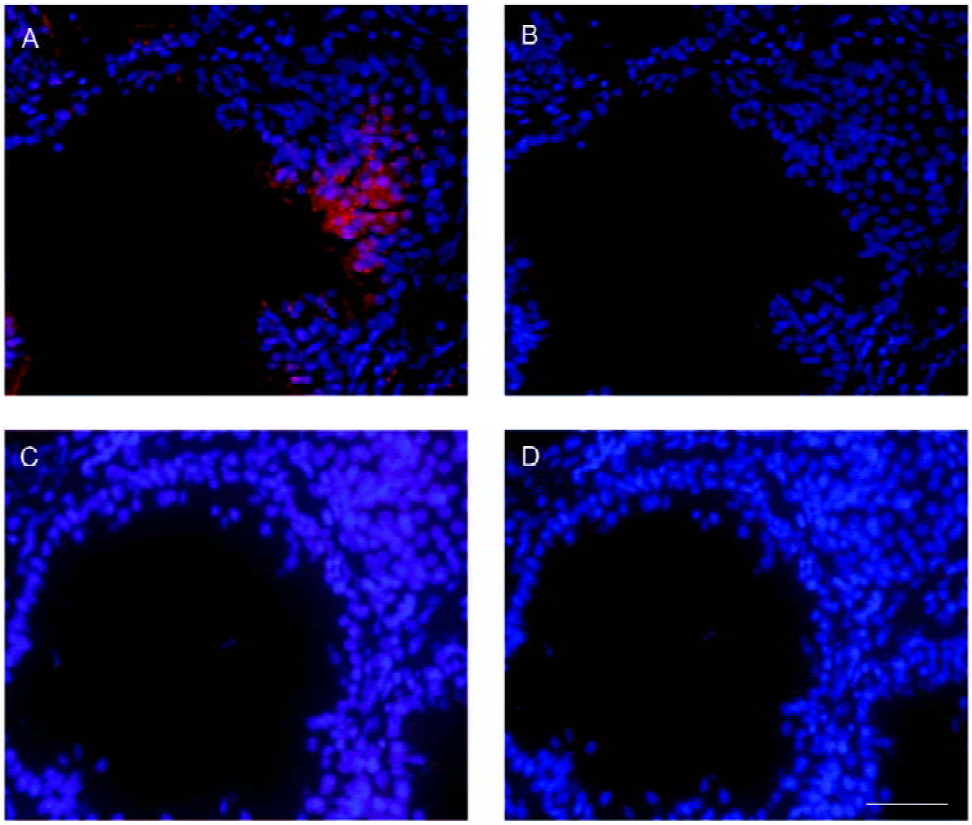

Figure 5. Immunofluorescence staining for TRPM8 (A) and TRPV1 (C) in rat prostatic tissues. Red areas indicate positive staining and denote negative controls without primary antibody (B and D). Blue areas represent nuclei stained with Hoechst 33258. Reduced from ×360. Scale bar = 10 μm.

results of Bidaux *et al.* [10]. The physiological role of TRPM8 as a cold receptor of the body has been revealed by an expression cloning approach to identify a menthol receptor from trigeminal neurons [11, 12]. The isolated cDNA codes for TRPM8 and forms a calcium-permeable cation channel. In TRPM8-expressing cells, application of menthol, icilin or other cooling agents induce TRPM8 currents, which are comparable to activation of TRPM8 by temperatures lower than 28ºC [13]. TRPM8 displays a cold receptor of the body, and its activation can be modulated by many cooling compounds and odorants. In addition, TRPM8 is an important determiner of Ca^{2+} homeostasis in prostate epithelial cells and might be a potential target for the action of drugs in the management of prostate cancer [14].

TRPM4 was found to be involved in the regulation of Ca^{2+} oscillations during T lymphocyte activation [15]. Recently, Fonfria and associates [16] observed the expression of TRPM4 in human prostate using TaqMan and SYBR Green real-time RT-PCR. The present study also confirms the existence of TRPM4 channel in rat prostate tissue.

Another finding of the present study was the abundant expression of TRPM2 and TRPM3 mRNA in prostatic tissue of rat. TRPM2 is highly expressed in the brain, and is also found in a variety of peripheral cell types [17]. It forms a nonselective cation channel permeable to mainly Na^+ and Ca^{2+}, as well as to K^+ and Cs^+. A long and a short splice variant, TRPM2-L and TRPM2-S, have been described [18]. Several diseases are linked to this gene, including a form of nonsyndromic hereditary deafness and holoprosencephaly [19]. TRPM3 forms a cation channel permeable to divalent cations, especially to Ca^{2+} and Mn^{2+} [20, 21]. TRPM3 is activated in response to activation of an endogenous muscarinic receptor by decreasing extracellular osmolarity. It has also been considered as a store-operated channel [20, 21]. TRPM3 expression has been demonstrated in kidney and brain, and at lesser levels in testis and spinal cord [20, 21]. No functional involvement of TRPM2 and TRPM3 has been established in prostatic disease.

In our results, there is little expression of TRPM6, TRPM7, TRPM1, and no expression of TRPM5. TRPM5 was found in the tongue, lungs, testis, digestive system, as well as in the brain [22]. TRPM5 channels in the taste receptor cells of the tongue appear essential for the transduction of sweet, amino acid (umami), and bitter taste [23]. Fonfria and associates [16] observed the expression of TRPM5 in human prostate using TaqMan and SYBR Green real-time RT-PCR. However, our study did not find any expression of TRPM5 with either traditional RT-PCR or real-time RT-PCR in five samples.

For the TRPV subfamily, our data indicate that TRPV4 and TRPV2 are the predominant transcripts expressed in rat prostate tissue. TRPV4 has been found widely expressed in the brain, dorsal root ganglion (DRG) neurons, and multiple excitable and non-excitable peripheral cell types [24]. We found that TRPV4 and TRPV2 are expressed in prostatic tissue of rat. The physiological functions of TRPV4 are thought to include central and peripheral thermosensing, mechano-sensing (including endothelial cell responses to shear stress), osmosensing, and basal Ca^{2+} homeostasis [24]. TRPV2 has been described as a stretch-activated channel, and has been found to mediate the hypotonic swelling-induced and stretch-induced increase in $[Ca^{2+}]i$ in vascular smooth muscle cells [25]. Expression of TRPV2 has been reported in the brain, and in some non-neuronal tissues and smooth muscle cells [26]. However, the functional significance of TRVP2 and TRPV4 in the prostate is still unclear. Further studies are required to address this point.

From our data, there is little expression of TRPV1, TRPV3, and no expression of TRPV5 and TRPV6. TRPV5 and TRPV6 are highly expressed in the kidney and intestine, respectively, where they form highly selective Ca^{2+} channels essential for Ca^{2+} reabsorption [27]. It is also demonstrated that TRPV6 is not expressed in benign prostate tissues, including benign prostate hyperplasia, but is upregulated in prostate cancer [28].

Here, we have identified a large repertoire of TRPM and TRPV channels in prostatic tissue of rat. In addition, we also found that some TRPM and TRPV channels are widely co-expressed in prostatic tissue. Our data might serve as the molecular and physiological basis for future explorations of the relation of TRP channels and prostatic disease. Further studies are required to investigate the diverse functions of non-selective ion channels in the prostate.

References

1 Xu XF, Zhou SW, Zhang X, Ye ZQ, Zhang JH, Ma X, *et al*. Prostate androgen-regulated gene: a novel potential target for androgen-independent prostate cancer therapy. Asian J Androl 2006; 8: 455–62.

2 Kang SH, Kim JW, Bae JH, Park HS, Moon DG, Yoon DK, *et al*. Targeted-cryosurgical ablation of the prostate with an-

drogen deprivation therapy: quality of life in high-risk prostate cancer patients. Asian J Androl 2006; 8: 629–36.
3 Catalona WJ, Smith DS, Wolfert RL, Wang TJ, Rittenhouse HG, Ratliff TL, *et al*. Evaluation of percentage of free serum prostate-specific antigen to improve specificity of prostate cancer screening. JAMA 1995; 274: 1214–20.
4 Murphy GP, Maguire RT, Rogers B, Partin AW, Nelp WB, Troychak MJ, *et al*. Comparison of serum PSMA, PSA levels with results of Cytogen-356 ProstaScint scanning in prostatic cancer patients. Prostate 1997; 33: 281–5.
5 Correale P, Walmsley K, Zaremba S, Zhu M, Schlom J, Tsang KY. Generation of human cytolytic T lymphocyte lines directed against prostate-specific antigen (PSA) employing a PSA oligoepitope peptide. J Immunol 1998; 161: 3186–94.
6 Murphy GP, Tjoa BA, Simmons SJ, Jarisch J, Bowes VA, Ragde H, *et al.* Infusion of dendritic cells pulsed with HLAA2-specific prostate-specific membrane antigen peptides: a Phase II prostate cancer vaccine trial involving patients with hormone-refractory metastatic disease. Prostate 1999; 38: 73–8.
7 Montell C. The TRP superfamily of cation channels. Sci STKE 2005; 3.
8 Yang XR, Lin MJ, McIntosh LS, Sham JS. Functional expression of transient receptor potential melastatin- and vanilloid-related channels in pulmonary arterial and aortic smooth muscle. Am J Physiol Lung Cell Mol Physiol 2006; 290: L1267–76.
9 Stein RJ, Santos S, Nagatomi J, Hayashi Y, Minnery BS, Xavier M, *et al.* Cool (TRPM8) and hot (TRPV1) receptors in the bladder and male genital tract. J Urol 2004; 172: 1175–8.
10 Bidaux G, Roudbaraki M, Merle C, Crepin A, Delcourt P, Slomianny C, *et al*. Evidence for specific TRPM8 expression in human prostate secretory epithelial cells: functional androgen receptor requirement. Endocr Relat Cancer 2005; 12: 367–82.
11 McKemy DD, Neuhausser WM, Julius D. Identification of a cold receptor reveals a general role for TRP channels in thermosensation. Nature 2002; 416: 52–8.
12 Peier AM, Moqrich A, Hergarden AC, Reeve AJ, Andersson DA, Story GM, *et al*. A TRP channel that senses cold stimuli and menthol. Cell 2002; 108: 705–15.
13 Behrendt HJ, Germann T, Gillen C, Hatt H, Jostock R. Characterization of the mouse cold-menthol receptor TRPM8 and vanilloid receptor type-1 VR1 using a fluorometric imaging plate reader (FLIPR) assay. Br J Pharmacol 2004; 141: 737–45.
14 Zhang L, Barritt GJ. Evidence that TRPM8 is an androgen-dependent Ca^{2+} channel required for the survival of prostate cancer cells. Cancer Res 2004; 64: 8365–73.
15 Launay P, Cheng H, Srivatsan S, Penner R, Fleig A, Kinet JP. TRPM4 regulates calcium oscillations after T cell activation. Science 2004; 306: 1374–7.
16 Fonfria E, Murdock PR, Cusdin FS, Benham CD, Kelsell RE, McNulty S. Tissue distribution profiles of the human TRPM cation channel family. J Recept Signal Transduct Res 2006; 26:159–78.
17 Kraft R, Harteneck C. The mammalian melastatin-related transient receptor potential cation channels: an overview. Pflugers Arch 2005; 451: 204–11.
18 Zhang W, Chu X, Tong Q, Cheung JY, Conrad K, Masker K, *et al.* A novel TRPM2 isoform inhibits calcium influx and susceptibility to cell death. J Biol Chem 2003; 278: 16222–9.
19 Nilius B, Voets T, Peters J. TRP channels in disease. Sci STKE 2005; 295: 8.
20 Nishida M, Sugimoto K, Hara Y, Mori E, Morii T, Kurosaki T, *et al*. Amplification of receptor signalling by Ca^{2+} entry-mediated translocation and activation of PLCgamma2 in B lymphocytes. EMBO J 2003; 22: 4677–88.
21 Rosker C, Graziani A, Lukas M, Eder P, Zhu MX, Romanin C, *et al*. Ca(2+) signaling by TRPC3 involves Na(+) entry and local coupling to the Na(+)/Ca(2+) exchanger. J Biol Chem 2004; 279: 13696–704.
22 Ullrich ND, Voets T, Prenen J, Vennekens R, Talavera K, Droogmans G, *et al*. Comparison of functional properties of the Ca^{2+}-activated cation channels TRPM4 and TRPM5 from mice. Cell Calcium 2005; 37:267–78.
23 Zhang Y, Hoon MA, Chandrashekar J, Mueller KL, Cook B, Wu D, *et al*. Coding of sweet, bitter, and umami tastes: different receptor cells sharing similar signaling pathways. Cell 2003; 112: 293–301.
24 Nilius B, Vriens J, Prenen J, Droogmans G, Voets T. TRPV4 calcium entry channel: a paradigm for gating diversity. Am J Physiol Cell Physiol 2004: 286: C195–205.
25 Muraki K, Iwata Y, Katanosaka Y, Ito T, Ohya S, Shigekawa M, *et al*. TRPV2 is a component of osmotically sensitive cation channels in murine aortic myocytes. Circ Res 2003; 93: 829–38.
26 Pedersen SF, Owsianik G, Nilius B. TRP channels: an overview. Cell Calcium 2005; 38: 233–52.
27 den Dekker E, Hoenderop JG, Nilius B, Bindels RJ. The epithelial calcium channels, TRPV5 & TRPV6: from identification towards regulation. Cell Calcium 2003; 33: 497–507.
28 Fixemer T, Wissenbach U, Flockerzi V, Bonkhoff H. Expression of the Ca^{2+}-selective cation channel TRPV6 in human prostate cancer: a novel prognostic marker for tumor progression. Oncogene 2003: 22: 7858–61.

Edited by Dr Gail S. Prins